# DESIGN AND DEVELOPMENT OF THE POINT-AHEAD ANGLE MECHANISM FOR THE LASER INTERFEROMETER SPACE ANTENNA (LISA)

**Simon Henein, Peter Spanoudakis, Philippe Schwab, Ivar Kjelberg, Laurent Giriens, Yvon Welte, Luca Dassa Ralf Greger*, Ulrich Langer***

*Centre Suisse d'Electronique et de Microtechnique (CSEM), Jaquet-Droz 1, 2002 Neuchâtel, Switzerland, peter.spanoudakis@csem.ch; +41 32 720 5111*

**RUAG Aerospace AG, Walisellen, Widenholzstrasse 1, 8304 Wallisellen, Switzerland*

## ABSTRACT

The Point Ahead Angle Mechanism (PAAM) for ESA's Laser Interferometer Space Antenna (LISA) mission will compensate the out-of-plane point-ahead angle between three satellites flying 5 million kilometres apart. The PAAM consists of a mirror supported by flexures allowing the mirror to rotate with a maximum stroke of ±1 mrad. The mirror is actuated in 0.14 µrad steps by two redundant linear Piezo LEGS® actuators driving a sine-bar. Since the actuators are self-locking, a special lever performing the role of a linear mechanical differential is used to provide redundancy. The design uses high-precision flexures to minimise mirror parasitic piston displacements in the picometres range. The angle is driven in closed loop using two capacitive sensors. This paper presents the mechanism at the design stage of an elegant breadboard (EBB) ready for tests. The performance requirements are summarized, then the overall concept of the mechanism is described, at last the key aspects of the detailed design are discussed: flexures design, kinematic structure, kinematic mount, redundant piezo-actuation, sensors and control. Optimisation of the design has shown that the selected high-precision design can meet the stringent requirements of fine positioning and severe environments.

## 1 INTRODUCTION

The objective of the Laser Interferometer Space Antenna (LISA) mission is to detect and observe gravitational waves from massive black holes and galactic binaries. A gravitational wave passing through the Solar System creates a time-varying strain in space that periodically changes the distances between all bodies in the Solar System. Gravitational waves will be observed by LISA using laser interferometry. The European LISA mission is composed of three identical spacecraft located at 5 million kilometres apart flying in an equilateral triangle formation rotating in a heliocentric orbit trailing the earth (Fig. 2). The plane of the three spacecraft is inclined by 60 degrees with respect to the ecliptic plane. LISA is basically a giant Michelson interferometer placed in space.

Each spacecraft will contain two reference targets, known as "proof masses", each of which acts as the end mirror of a single-arm interferometer. The passage of gravitational waves will be measured by observing combinations of the movements of the proof masses, and thus arm length changes. The LISA interferometric measurement system has to provide an absolute accuracy in the range of 10 pm/√Hz for a single arm laser link, given an arm length of $5 \times 10^6$ km. The plane circumscribed by the three spacecraft constitutes a very large gravitational-wave antenna.

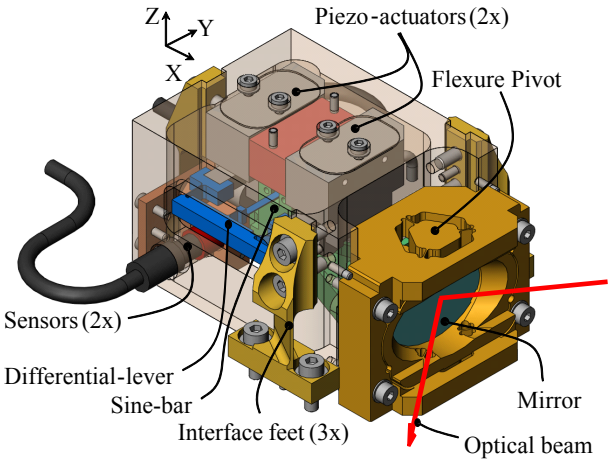


*Figure 1. Transparent CAD view of the PAAM mechanism*

The accurate determination of arm length variations is complicated by the fact that the shape of the formation triangle undergoes residual seasonal changes, which cannot be completely removed by orbit optimization. These changes not only affect the nominal 60°angle between the lines of sight (LOS), but also the so called point-ahead angle, which describes the offset between received and transmitted beam for each individual spacecraft. This offset is required to account for the comparatively long travel time of the laser light to the respective remote spacecraft, which is approximately 16 seconds.

The Point Ahead Angle Mechanism (PAAM), Fig. 1, will compensate the out-of-plane point-ahead angle between the three satellites. The mechanism was designed and developed jointly by CSEM (CH) and RUAG Aerospace (CH) and is currently undergoing tests. The objective of the project is to design, develop,

test and validate an elegant breadboard (EBB), see Fig. 3, of the PAAM with a design maturity ready to enter directly into the LISA implementation phase.

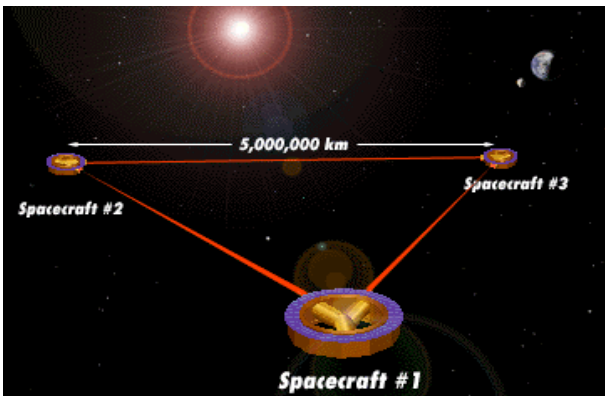


*Figure 2. LISA spacecraft orientation in orbit around the sun (www.esa.int)*

## 2 GENERAL PERFORMANCE REQUIREMENTS

The PAAM is a critical item as it is positioned on the optical bench, directly in the measurement path. Any dimensional change due to the actuator jitter, misalignment, small thermal gradients or mechanical stress will be seen as a pathlength change at the interferometer output. For this reason, mechanical and thermal stability, including that of the interfaces to mount the mechanism onto the optical bench are critical. Particularly critical is, the parasitic "piston" motion of the mirror (i.e. the translation perpendicular to the mirror surface) that might accompany its rotation, since it is directly seen by the system as a pathlength error.

Technically, the critical design requirements for the PAAM are:

- Angular stroke : ± 412 µrad (mechanical angle)
- Scanning speed : ± 62.5 prad/s (this extremely low value leads to a scanning time of 155 days to cover the entire angular range)
- Scanning error at any time should be below ± 4 µrad
- longitudinal pathlength stability $1.4\frac{pm}{\sqrt{Hz}}\sqrt{1+\left(\frac{2.8mHz}{f}\right)^4}$
- Maximum pointing jitter below $8\frac{nrad}{\sqrt{Hz}}\sqrt{1+\left(\frac{0.0028}{f}\right)^4}$ in the frequency band between $10^{-4}$ Hz and 1 Hz (mechanical angle)
- Total Piston error of <1.5 pm for a 0.14 µrad rotation
- Design loads of 75 g
- Use of non-magnetic material and components
- Stringent cleanliness requirements

## 3 MECHANISM'S GENERAL DESCRIPTION

The concept of the mechanisms relies on flexure structure technology (FLEXTEC) developed by CSEM over more than two decades [3]. With this approach, high-accuracy guiding is possible without the need for sliding surfaces or rolling bearings. One of the particularities of the presented approach is that the system is operated in a quasi-static open loop mode. The actuators selected are blocked most of the time and the stability relies mainly on the mechanics and to a lesser extent on the electronic noise of the sensors. The drawback is that it operates in larger discrete steps, but these are performed within a short time period (msec).

The general architecture and functionality of the PAAM mechanism (mass 160 g, 73x56x36 mm) is described below.

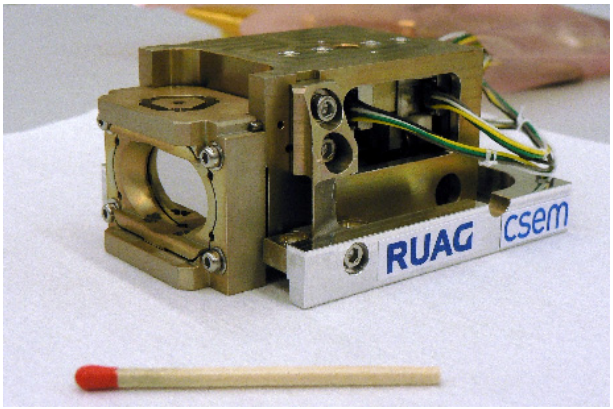


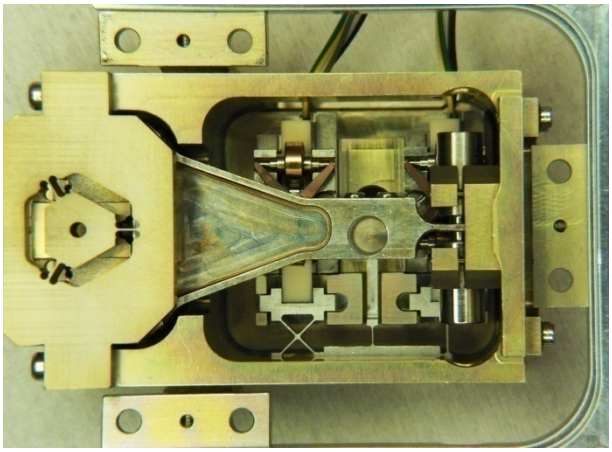

*Figure 3. Photos of the PAAM Mechanism EBB*

### 3.1 Flexure pivot

The optical mirror is supported by a monolithic flexure pivot with a motion range of ±412 µrad. To get a rotation that is devoid of any parasitic shifts [2] and that is very stiff in the piston direction (X), two identical concomitant three-blade flexure pivots are used, one on each side of the mirror (Fig. 4). The pivot is cut monolithically by high-precision Wire Electrodischarge-

machining (EDM) in Aluminium alloy 6061-T651. The blades that are placed at 120 degrees to one another lead to an over-constrained arrangement (two blades already constitute a 1 degree-of-freedom (DOF) pivot). This is acceptable in the current application since the angular range is extremely reduced. The pivot has been designed taking into account its machinability and maximising the optical beam clearance (Fig. 5).

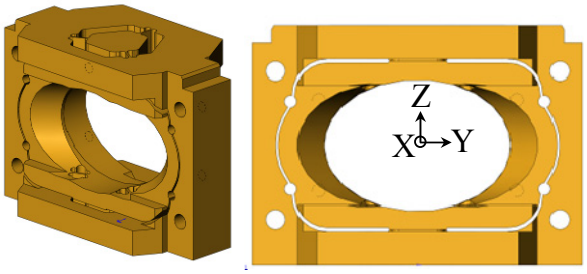


*Figure 4. PAAM flexure pivot and mirror support*

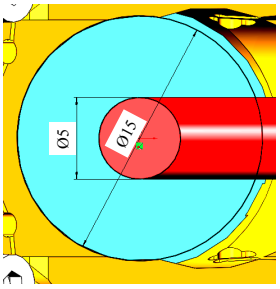


*Figure 5. Optical beam-clearance, 3X beam diameter*

### 3.2 Sine-bar and differential-lever for redundant actuation

The flexure pivot is driven by a sine-bar attached to it. The sine-bar is actuated by two redundant piezoleg-actuators acting through a differential-lever (Fig. 6 & 7). Each of the two extremities of the differential-lever is attached to one piezoleg-actuator via a flexure pivot. The mid-point of the differential lever is attached to the sine-bar via a decoupling arm, at a distance of 36 mm from the rotation axis of the mirror. To move the sine-bar over a distance $Y = 15\ \mu m$, the main actuator has to move twice as much: $Y1 = 2\ Y = 30\ \mu m$. To be able to move the sine-bar over a distance Y while the main actuator is blocked at any position along its range due to a failure, the secondary actuator needs to be able to move over a range that is double: $Y2 = 2\ Y1 = 4\ Y = 60\ \mu m$ . Like the torque on both ends of a classical mechanical differential based on gears, the forces on both ends of the differential lever are always equal. Moreover, the displacement at the mid-point of the lever is one half of the displacement made by any of the actuators (actuated individually). For that reason this driving mechanism has been called "differential-lever".

The idealized planar kinematic structure shown on top of Fig. 6 is composed of 8 1-DOF joints (i.e. it has a Mobility of 8) and 2 closed kinematical loops. Therefore, according to Grübler's kinematical criterion [1] for planar linkages, the structure has

$$8 - 2 \cdot 3 = 2 \text{ DOF}.$$

Each of those DOF is driven by one actuator. Due to the selected dimensions, the effects of both actuators are identical at the mirror level.

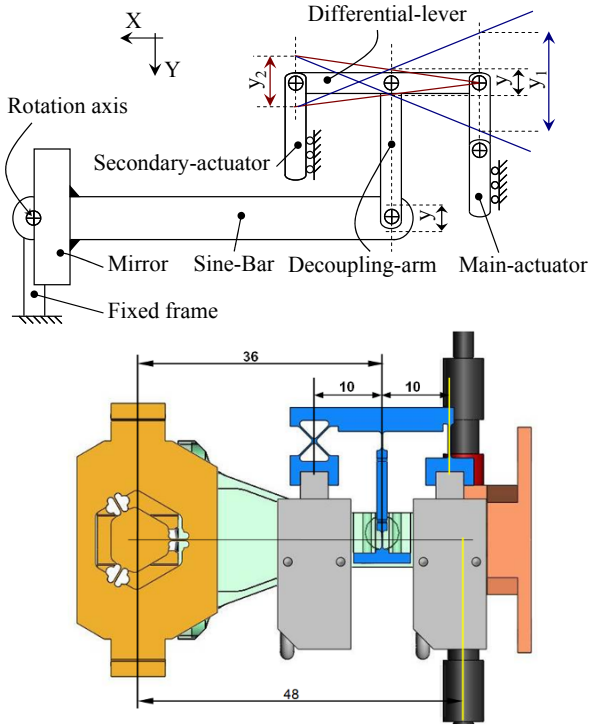


*Figure 6. Kinematic chain from mirror to actuator. Top-down: schematic representation, CAD model and differential-lever unit alone.*

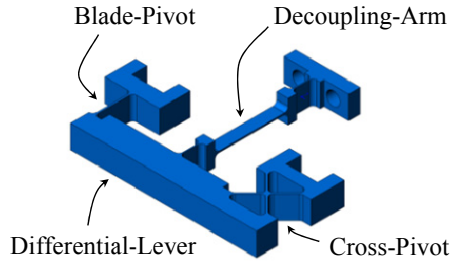


*Figure 7. Differential-lever unit (3mm thick plate)*

The role of the decoupling arm is to transmit a pure force to the sine-bar that is perpendicular to it. Indeed, the parasitic forces and torques applied to the sine-bar need to be minimised to avoid parasitic motions (in particular "piston" along X) of the mirror.

### 3.3 Piezo-actuators

Two redundant piezo stepping actuators are used to drive the mechanism (Fig. 8). The selected commercial actuators are non-magnetic, UHV compatible versions of the Piezo LEGS®, multiple bimorph actuators. Those are co-sintered to a single body with four movable legs made out of ceramic "muscles". A driving leg can be considered as a piezoceramic bimorph. It is possible to activate each layer independently of the other by an electric voltage. Step sizes ranging from 10 nm to 80 nm are used. When they are powered-off, those actuators are self locking, i.e. the failure of one actuators leads to a blocking of the respective degree-of-freedom (DOF) of the mechanism. Therefore, to achieve the required redundancy, a two DOF kinematical chain is required to link the two actuators to the rotating mirror. This function in fulfilled by the Differential-Lever and the Sine-Bar.

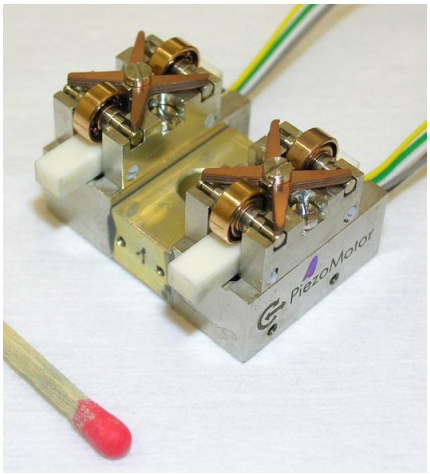


*Figure 8. Photo of the two Piezo LEG actuatrors*

### 3.4 Sensors

The rotation angle of the mirror is measured by two capacitive sensors measuring the linear displacement of the mobile extremity of the Sine-Bar in differential mode. MicroEpsilon S601-0.05 capacitive sensors are integrated as a baseline in the current design (Fig. 9). The MicroEpsilon CS02 has similar performance and might be preferable from an electronics point of view since it has a larger measurement area (diameter of 5 mm instead of 3 mm). The latter product is kept as a backup solution.

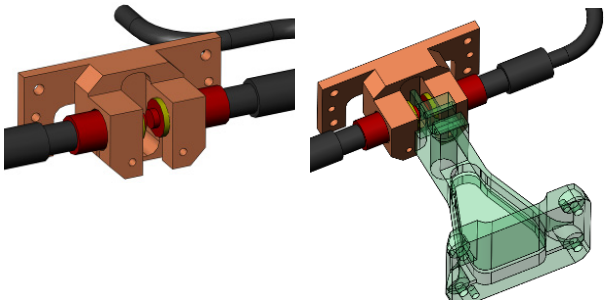

*Figure 9. Capacitive sensors and target at the extremity of the Sine-Bar.*

### 3.5 Phase B Breadboard prototype

The mechanism is attached to the optical bench by three flexible feet that constitute a kinematic mount. The elastic region of the feet is a simple blade. The three feet are oriented so that the three lines that stem perpendicularly to each blade meet in one point, called the geometrical-centre of the mount. Due to volume constraints, the feet could not be placed in a symmetrical arrangement with respect to the geometrical-centre as it is usually done with such assemblies. Consequently, the thermal-centre of the mechanism does not exactly coincide with the geometrical-centre (Fig. 10). This offset is due to the fact that the sum of the elastic forces exerted onto the mechanism by the feet (out-of plane natural bending) when homogeneous thermal expansion takes place is not zero. The resulting force then deforms the elastic feet in their transverse direction (in-plane bending) causing a slight shift of the mechanism. In the present design, the offset between the geometrical and thermal centres of 1.05 mm provides a near zero thermal offset.

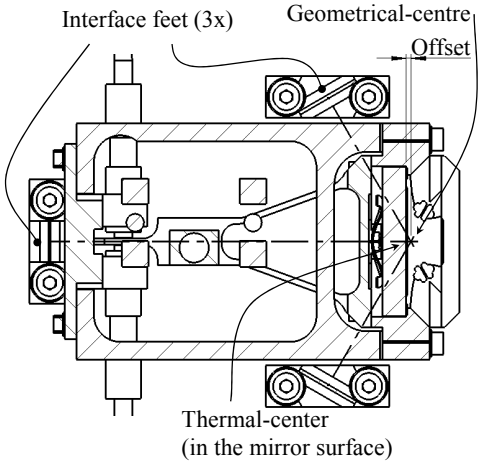


*Figure 10. Arrangement of the three isostatic feet and corresponding geometrical and thermal centres.*

The rotation centre of the main flexure pivot passes through the thermal-center of the mechanism. The mirror is referenced to the mechanism from its front-

side so that the rotation axis of the pivot and the thermal-centre lies within its optical surface.

The three isostatic feet are pin-screwed to titanium (Ti6Al4V) support blocks that are bonded with epoxy to the Zerodur optical bench (no inserts are allowed in the optical bench). The use of titanium as an interface material (instead of aluminium as the rest of the mechanism) allows a significant reduction of the thermo-elastic stresses in the optical bench due to differential thermal expansion (ΔT of up to 60°K). See section 4.5.

The nominal height of the optical beam is 15 mm above the surface of the optical bench. The PAAM mechanism, including its feet is separable from the optical bench. Only the three titanium blocks remain permanently bonded on the bench.

## 4 DETAILED ANALYSIS

### 4.1 FEM analysis of the flexure pivot

In a first stage, an ideal FEM model of only the six flexible blades was calculated with the rest of the structure considered infinitely stiff (Fig. 11). Identical meshing (full symmetry) has been used in all blades in order to avoid the inherent errors that would result from automatic meshing. The pivoting accuracy level we are looking for is sensitive to parasitic effects due to differences in apparent stiffness in each blade.

This simplified FEM model (Fig. 12, IDEAL pivot) was also used to validate the analytical results before moving onto the integrated model with its structural parts. Both models agreed very well. The simulations were carried out using NASTRAN and COMSOL and allowed CSEM to validate and verify coherence of results between the two software tools.

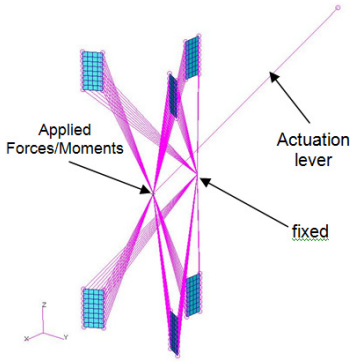


*Figure 11. The simplified flexure pivot analysis considers only the flexure blades. The rest of the structure is considered infinitely stiff.*

In a second stage, the complete flexure pivot has been modelled by FEM. This model includes the same flexure blades as in the simplified case but integrates the surrounding support structure of the pivot and actuating levers (Fig. 12, top). These simulations show that the role of the stiff structure holding the flexible blades is by no means negligible (Fig. 12, REAL column). In particular the translation stiffnesses of the pivot in the X, Y and Z directions are strongly affected by the non-infinite stiffness of the rigid structure: 64% to 72% of the compliance (which should ideally be zero) in these directions result form the flexibility of the "rigid" structure of the pivot and only the remaining 27% to 35% result from the elastic blades themselves.

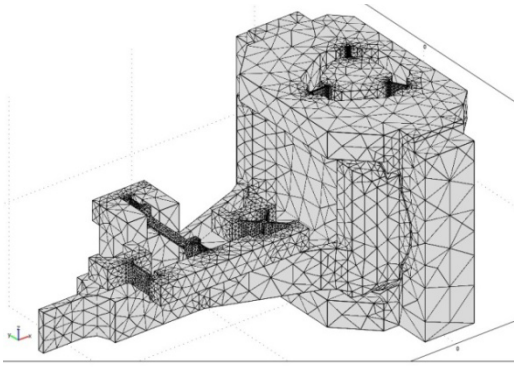

| **FEM results** | **IDEAL pivot** | **Pivot & Structure** |
|---|---|---|
| Equivalent spring rotational stiffness of all 6 blades | **82 Nm/rad** | **79 Nm/rad** |
| **Linear stiffness** | | |
| X-direction | **97 N/µm** | **27 N/µm** |
| Y-direction | **97 N/µm** | **34 N/µm** |
| Z-direction | **56 N/µm** | **16 N/µm** |

*Figure 12. Complete FEM of the flexure pivot and numerical results without and with structure.*

### 4.2 Structural analysis of the isostatic feet

The worst case loading condition of 75g quasistatic load in the Y-direction leads to maximum stresses of 204 MPa in the isostatic feet (Fig. 13). This stress level is acceptable for the high strength aluminum alloy 7075-T7351 that has an ultimate strength of 495 MPa.

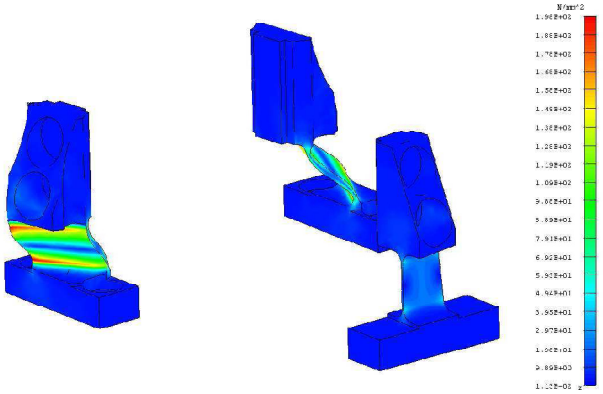

*Figure 13. Stress distribution in interface feet with quasistatic loading in the Y-direction*

### 4.3 Modal analysis

The modal analysis confirmed that the first mode at 425 Hz (Fig. 14) was significantly above the minimum frequency of 125 Hz.

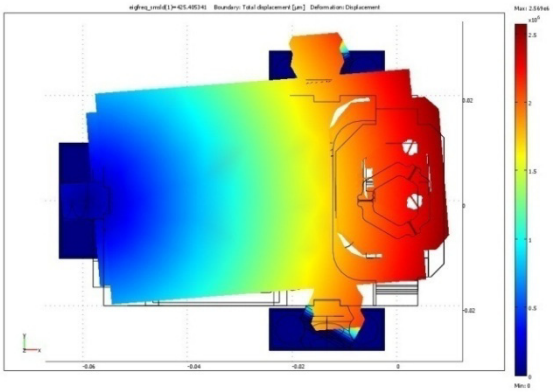

*Figure 14. The first eigenfrequency at 425 Hz*

### 4.4 Piston effect due to thermal variation

It has been determined, through iterative FEM simulations that in order to obtain a thermal shift close to zero within the operative condition temperature stability ($1x10^{-5}$ K/√Hz), the required offset between the geometrical and thermal centres of the mechanism (Fig. 10) is 1.05 mm.

### 4.5 Thermo-elastic analysis

The temperature range taken into account for the thermal analysis considers the worst case upper limit (+80°C during bake out) from the reference temperature of +20°C.

The initial thermo-elastic stresses on the optical bench were excessively high due to dissimilar materials (Al feet and Zerodur bench), the surface area of the interface feet and the large temperature range considered (Δ60°). A change in the material of the support blocks from Al 7075 to Titanium alloy was implemented in order to reduce the stresses on the optical bench (Fig.15). The stresses on the optical bench with the Titanium support blocks including a 150µm epoxy layer were significantly reduced (from 200 MPa to 25 MPa) when compared to the Aluminium blocks.

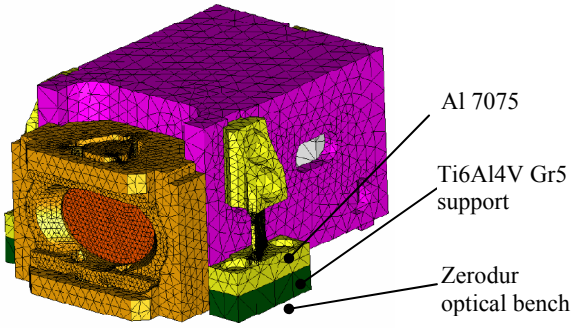


*Figure 15. FEM model with Ti support blocks at I/F*

### 4.6 Piston error resulting from actuation parasitic loads

The differential-bar unit should exert a pure torque onto the Sine-Bar to get a pure rotation of the flexure pivot. In reality it is applying a normal force at the extremity of the Sine-Bar, plus some parasitic forces and torques resulting from the residual stiffnesses of the Decoupling-Arm. Those parasitic effects cause some complex parasitic motions of the mirror.

Only the major and most critical contribution is discussed here. It is the parasitic force exerted axially (i.e. in the X direction) on the Sine-Bar by the Decoupling-Arm. Indeed, this force directly results in a piston motion of the mirror and contributes to the longitudinal pathlength stability error.

Two cases have been considered for the actuation of the flexure pivot over its full stroke:

In the nominal case, the actuator pushes the lever by ± 35 µm to obtain the full rotational scan of the pivot to ± 412 µrad. In that case an axial parasitic force of ± 1.5 N acts on the Sine-Bar, which results in a parasitic piston motion of the mirror (X direction) of ± 55 pm.

In the worst case, the main actuator is presumed to have failed in one of its extreme positions (35 µm). The secondary then has to move 70 µm in the opposite direction to bring the mirror to its worst-case extreme angular position of 412 µrad. In that case, an axial parasitic force of 6.5 N acts on the Sine-Bar, which results in a parasitic piston motion of the mirror (X direction) of 240 pm.

Two other cases have been considered for micro-step motions of the actuator:

In nominal functional mode, one actuator makes a 10 nm step and the mirror rotates 0.14 µrad. The resulting theoretical piston error at the mirror level is 0.018 pm ($18 \cdot 10^{-15}$m). If the main-actuator fails at one of its extreme position, then a step of 10 nm of the secondary actuator results in a rotation of 0.14 µrad of the mirror plus a piston error of 0.08 pm.

The piston error budget at mechanism level has been translated from an error as a function of frequency based on a scanning speed of 62.5 prad/sec. The allocated piston error budget for a 0.14 µrad step is 1.5 pm. The maximum piston error (statistical sum) for a 0.14 µrad step rotation of the mirror is 0.88 pm (error contribution includes pivot rotation errors, manufacturing tolerance, material property variation and isostatic interface thermal offset error).

### 4.7 Stress in flexures during nominal deflections

For the nominal scan range of 412 µrad, the maximum stress in the mirror flexure pivot is 19 MPa. The

corresponding stress in the cross-spring-pivot of the Diffrential-Bar is 10 MPa. The corresponding stress in the blade-pivot of the Diffrential-Bar is 5 MPa. In the worst case situation, where the main actuator fails in one of its extreme positions, the maximum stress in the structure reaches 32 MPa and is located at the cross-spring-pivot of the Diffrential-Bar).

In order to have an operational margin and sufficient end of travel range, the maximum acceptable rotation of the flex pivot has been fixed to ±1000 µrad. The corresponding stresses for this displacement are 44 MPa in the mirror flexure pivot, 24 MPa in the cross-spring-pivot of the Differential-Bar and 12 MPa in the blade-pivot of the Differential-Bar.

## 5 TESTS (COMPONENTS LEVEL)

The proposed components (actuator, sensor, flexure hinge) have been tested at component level as well as in a development model (Fig. 16). The principal validity of the baseline design and its components was verified and confirmed.

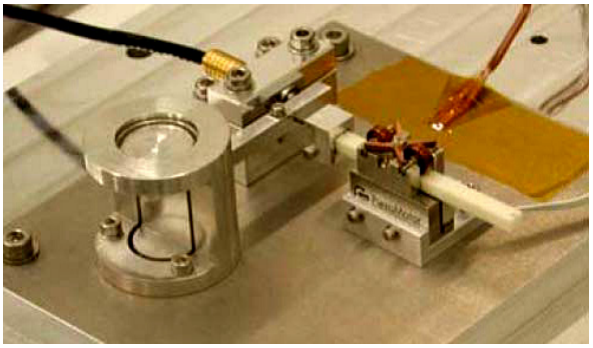

Figure 16. Development model to test the components

### 5.1 Control

In order to track the nominal reference of 62.5 prad/s, the mirror is periodically moved of an angle $\Delta\alpha$ and subsequently blocked for a duration of $\Delta T$ as illustrated in Figure 17.

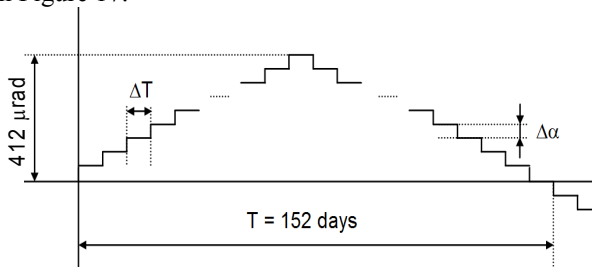


*Figure 17. Stepwise motion of the mirror*

Tests were performed using the development model (DM) to evaluate the effect of step sizes on sensor noise stability. The DM stability was analysed while moving the actuator along the nominal scan speed and varying step sizes (Fig. 18).

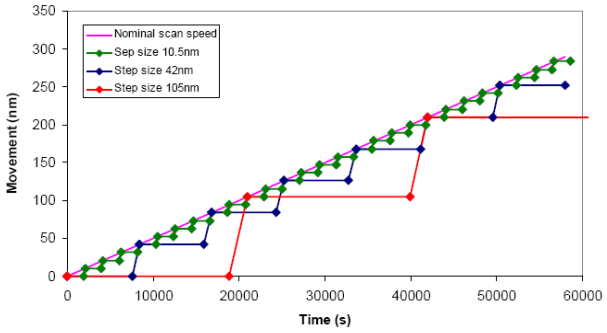


*Figure 18. Stepwise scan speed approach with ramp*

### 5.2 Power dissipation

The average power dissipation of the actuators was measured below 1 mW during the nominal operational scanning mode. The power dissipation of the position sensor pair will be approximately 2 mW according to the manufacturer. The maximum power dissipation of 10 mW will not be exceeded.

## CONCLUSION

A redundantly actuated, high stability tilt mirror concept for the LISA PAAM has been designed, prototyped and tested. The tilt range exceeds the specified ±412 µrad and meets the stringent piston error or pathlength stability requirements well within the power consumption budget.

Extensive simulations and design effort has been utilised to minimise stress levels and optimise the stability of the device to reach the pico-metre level pointing noise performance required. High stability is obtained by relying on precision compliant mechanics machined by EDM and operated with a stiff actuator in quasi-static open-loop stepping mode.

A comprehensive test campaign has started at RUAG (CH) to evaluate functional performance and environmental tests of the EEB mechanism. Additional performance tests (jitter and longitudinal stability) over temperature range will take place at AEI Hannover (D).

## ACKNOWLEDGMENTS

The authors would like to thank:

- Mecartex SA for the precision EDM machining.
- L. Rossini (CSEM) and L. Scolamiero (ESTEC)

## REFERENCES

[1] Grübler, *Getriebelehre*, Berlin: Springer, 1917

[2] S. Henein, et. al., *Flexure Pivot for Aerospace Mechanisms*, Proceedings of the 10th ESMATS, ESA SP-524, 2003

[3] L. Zago, et. al., *Advanced Flexure Structures in Active High-Accuracy and Large Bandwidth Mechanisms*, SMACS, 1997